International Geology Review, Vol. 43, 2001, p. 624–639.

Petrology of the Kurancali Phlogopitic Metagabbro: An Island Arc–Type Ophiolitic Sliver in the Central Anatolian Crystalline Complex

FATMA TOKSOY-KÖKSAL, M. CEMAL GÖNCÜOGLU,

Department of Geological Engineering, Middle East Technical University, TR-06531, Ankara, Turkey

AND M. KENAN YALINIZ

Department of Civil Engineering, Celal Bayar University, Manisa, Turkey

Abstract

The Kurancali metagabbro occurs as an isolated body in the central part of the Central Anatolian Crystalline Complex. It has been emplaced along a steep S-vergent thrust-plane onto the uppermost units of the Central Anatolian Metamorphics. The main body of the Kurancali metagabbro is characterized by distinct compositional layering. The layered gabbros comprise pyroxene and hornblende gabbros. Phlogopite-rich, plagioclase-hornblende gabbro occurs mainly as pegmatitic dikes intruding the layered gabbro sequence. The layered gabbros, in general, consist mainly of diopsidic augites, brown hornblendes, and plagioclase. Secondary phases are phlogopitic mica, brownish-green hornblende replacing clinopyroxenes, and fibrous, greenish actinolitic hornblende partially or completely replacing brown hornblende. The primary dark micas are phlogopitic in the range of $phlogopite_{(57-70)}$ and $annite_{(30-43)}$. The analyzed pyroxenes are diopsidic ($En_{32}Fs_{19}Wo_{49}$-$En_{35}Fs_{18}Wo_{48}$).

The whole-rock geochemistry of the gabbros indicates the presence of two distinct groups of rocks; a less pronounced group of phlogopite gabbro with island-arc calc-alkaline affinities, and a dominating layered gabbro sequence with island-arc tholeiite characteristics. They are extremely enriched in LILE, indicative of alkaline metasomatism in the source region, and display geochemical features of transitional backarc-basin basalts (BABB)/island-arc basalts (IAB)—and IAB-type oceanic crust. Based on their geochemical similarities to modern island-arc basements, we suggest that the Kurancali metagabbro may represent the basement of an initial island arc, generated in a supra-subduction zone setting within the Izmir-Ankara branch of Neotethys.

Introduction

A PROMINENT ASSEMBLAGE of magmatic and metamorphic rocks that crops out in Central Anatolia (Fig. 1) is the Central Anatolian Crystalline Complex (CACC)—the topic of numerous studies (e.g., Göncüoglu et al., 1991, 1992, 1993, 1998; Göncüoglu and Türeli, 1993, Yaliniz et al., 1996). According to these authors, the CACC comprises the Central Anatolian Metamorphics, the Central Anatolian Ophiolites (CAO) that are thrust over the metamorphics, and the Central Anatolian Granitoids that intrude both units (Fig. 1C).

In the CACC, despite the more or less ordered ophiolitic bodies with preserved magmatic pseudostratigraphy, many massive and layered gabbroic rocks occur as isolated outcrops (Yaliniz and Göncüoglu, 1998). Except for a few outcrops of gabbroic rocks that have been interpreted as intrusive assemblages within the CACC continental crust (Yilmaz-Sahin and Boztug, 1997; Kadioglu et al., 1998), most of these mafic rocks have been accepted as dismembered parts of an allochthonous ophiolitic assemblage (Göncüoglu et al., 1992; Yaliniz et al., 1996; Yaliniz and Göncüoglu, 1998; Floyd et al., 2000), derived from the northerly Izmir-Ankara branch of the Alpine Neotethys. An overall supra-subduction zone genesis has been accepted for the CAO. However, remarkable differences in the geochemical characteristics of different isolated outcrops suggest differences in source areas and tectonic settings within the intra-oceanic subduction zone.

In this study, an isolated gabbro exposure around Kurancali (Kaman-Kirsehir) will be discussed. The characteristic feature of the Kurancali metagabbro is the presence of dark phlogopitic mica. In this

0020-6814/01/540/624-16 $10.00.

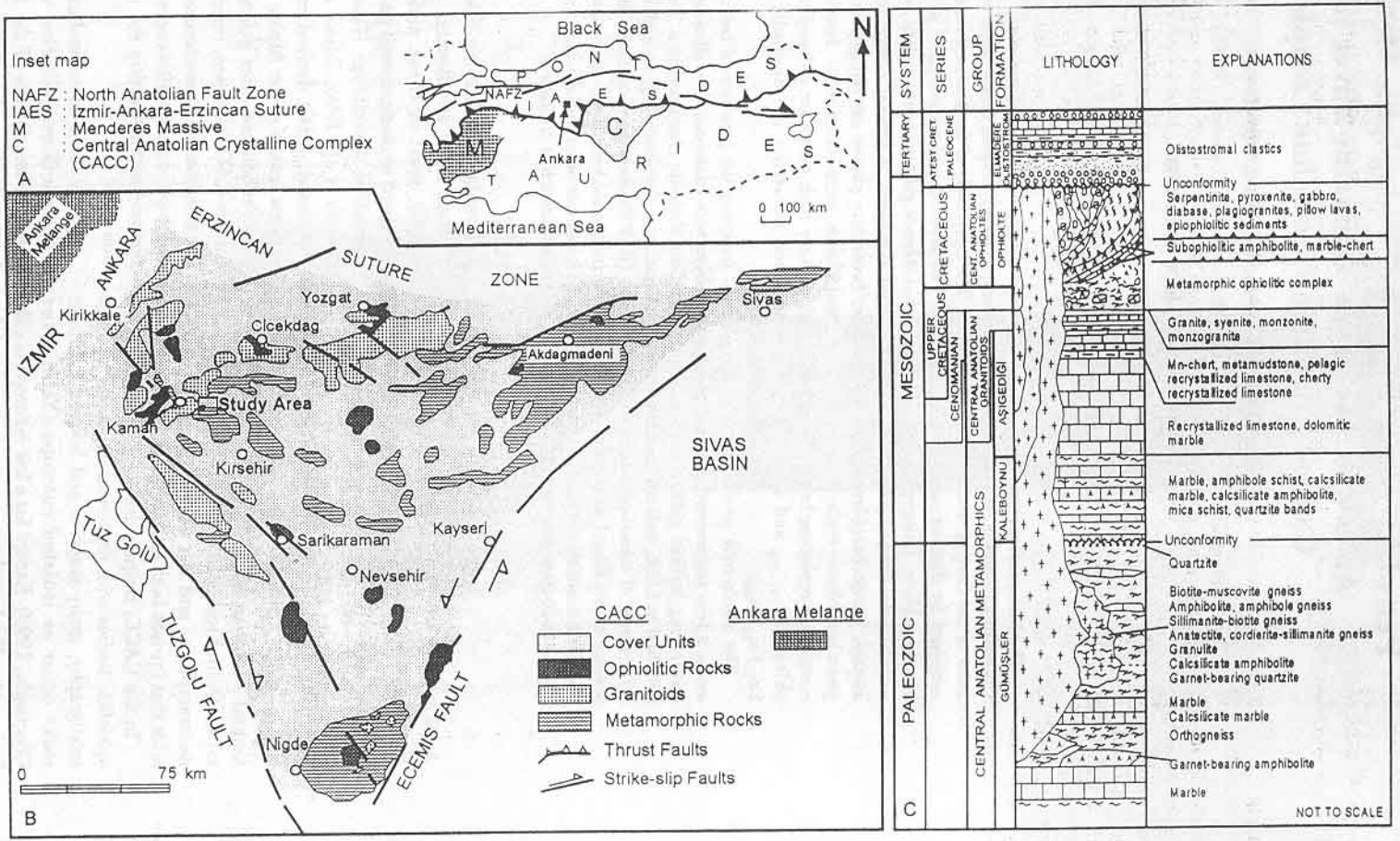

FIG. 1. Tectonic setting, geology, and rock units of CACC. A. Location of CACC in the tectonic framework of Turkey. B. Simplified geological map of CACC showing the geological settings of the main units and location of the study area (after Yaliniz and Göncüoglu, 1998). C. Generalized columnar section of the CACC (modified from Göncüoglu et al., 1991).

respect, the Kurancali metagabbro differs from other mafic and ultramafic rocks of the CAO.

The occurrence of phlogopite in mafic and ultramafic rocks has been the subject of copious studies (Hawkesworth and Norry, 1983; Arculus, 1994, and references therein). These studies were focused mainly on phlogopite-bearing xenoliths in volcanic rocks. It has been shown that metasomatism by either silica-rich fluids or hydrous melts, derived from the subducting slab and/or the hanging-wall mantle, were responsible for the crystallization of phlogopite. Thus, the role of a "subduction component" has been widely accepted. However, the occurrence of phlogopite is reported not only in arc-related settings, including forearcs, arc basements, and backarcs, but also in intra-continental potassic magmatic rocks. Therefore, we studied the whole-rock and mineral chemistry of these phlogopite-bearing gabbros and compared their overall geochemical characteristics with rocks from better-constrained tectonic settings—mainly with those in the CACC—to decipher their tectonic setting during the closure of the Izmir-Ankara seaway.

Geology

The Kurancali metagabbro occurs as a tectonic sliver to the east of Kaman (Kirsehir) in central Anatolia. It tectonically overlies the uppermost unit of the Central Anatolian Metamorphics along a steep, E-W–trending, shear zone (Fig. 2). The underlying metamorphic complex is a metamorphic olistostrome with blocks of ophiolitic rocks and metacarbonates. In the study area, the metamorphic olistostrome is dominated by irregular bands and lenses of calc-silicate amphibolite, calc-silicate marble, cherty marble, amphibolite, and metaserpentinite within a matrix dominated by calc-silicate–biotite gneiss and amphibole-biotite gneiss. The amount of calc-silicate rock diminishes, whereas the amphibole-biotite gneiss increases away from the underlying metacarbonate contact. The intervening shear zone, between the Kurancali metagabbro and the metamorphic ophiolite-bearing olistostrome, is characterized by the presence of highly sheared boudins of metagabbro, amphibolite, and metaserpentinite boudins.

Dikes of the Kurancali Granitoid, made up of alkali-feldspar granite, quartz syenite, and alkali-feldspar syenite, cut tectonic slices of the Kurancali metagabbro, the metamorphic ophiolite-bearing olistostrome, and the shear zone in an approximately NW-SE direction. The dikes exhibit sharp contacts with the host rocks, and are moderately sheared.

The layered Kurancali metagabbro shows heterogeneity in both composition (leuco- to melano-) and in grain size (fine-grained to pegmatitic). On the basis of modal mineralogy, three major gabbro types have been identified in the field—pyroxene gabbro, hornblende gabbro, and phlogopite gabbro (Fig. 2).

The pyroxene gabbro is either massive or layered. The layered pyroxene gabbro mainly shows rhythmic alternations of pyroxene and plagioclase. Massive pyroxene gabbro is characterized by the absence of plagioclase. Primary hornblende in the pyroxene gabbro is not abundant, although it is dominant within the fine-grained pyroxene gabbro, either as pegmatitic enclaves or irregular layers. This rock type is mainly composed of dark hornblende with lesser amounts of plagioclase. Typically, the hornblende gabbro is associated with large, prismatic pegmatitic hornblende crystals (up to 20 cm in length), and has plagioclase-dominated leucocratic phases.

The irregular masses of coarse-grained (pegmatitic) phlogopite gabbro consist mainly of phlogopite with lesser amount of pyroxene. The phlogopite crystals are blackish and have diameters of up to 2.5 cm. Almost no plagioclase is present in the phlogopite gabbro. In addition, the presence of hornblende is restricted to neighboring hornblende gabbro. The phlogopite gabbro is generally fresh; however, in some outcrops, the phlogopites are altered to gold-yellow vermiculite.

Petrography

The Kurancali metagabbro is essentially composed of varying amounts of clinopyroxene, phlogopitic mica, hornblende, and plagioclase. The rock samples also have secondary hornblende (uralite), actinolitic hornblende, vermiculite, albite, sericite, and rarely epidote. The accessory minerals of the metagabbro are titanite and magnetite-hematite. Although the Kurancali metagabbro is divided into three main types for field purposes, detailed petrographic investigation revealed the following types: phlogopite gabbro, pyroxene-phlogopite gabbro, pyroxene gabbro (pyroxenite), pyroxene-hornblende gabbro, pyroxene-plagioclase gabbro, hornblende gabbro, hornblende-plagioclase gabbro, plagioclase-hornblende pegmatitic gabbro, and hornblende-plagioclase pegmatitic gabbro.

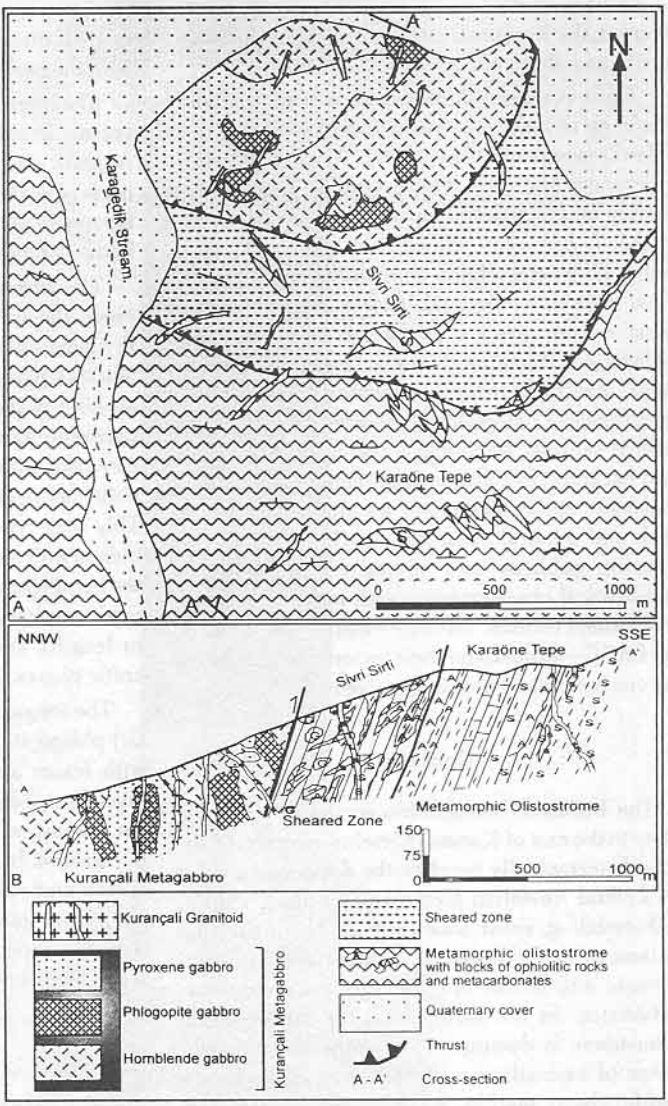

FIG. 2. A. Geological map of the study area. B. Cross-section of the study area showing the rock units and their contact relationships.

In general, although altered to varying degrees, the Kurancali metagabbro exhibits well-preserved igneous textures, plastic deformation, and cataclasis. The gabbros are characterized by a cumulus texture that is especially well preserved in the pyroxene gabbro. Cataclastic and mylonitic textures are also recognized by crystal bending (especially in micas), granulation, and brecciation.

The most abundant mineral of the Kurancali metagabbro is colorless to pale green or pale greyish green diopsidic augite. The augite occurs as very fresh, euhedral, short prismatic grains to intensely altered, fractured, and fragmented anhedral ones (Fig. 3A). Augite is commonly replaced by secondary hornblende and dark mica at rims, and along cleavage and fracture planes.

Hornblende, one of the major phases, is the primary magmatic mineral in hornblende gabbro, hornblende-plagioclase gabbro, and plagioclase-hornblende gabbro. Primary hornblende usually

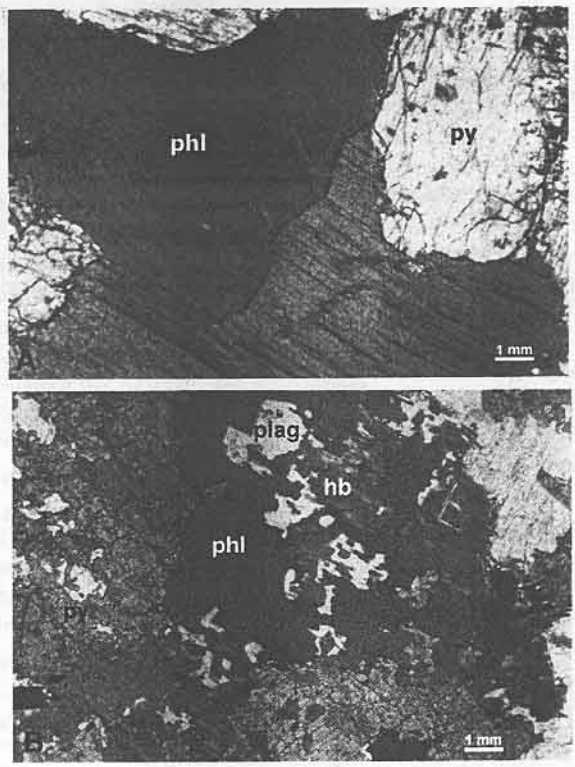

FIG. 3. Photomicrographs of the pegmatitic gabbro showing the relationships of: (A) clinopyroxene and primary phlogopite; (B) clinopyroxene, relic hornblende, and phlogopite replacing hornblende and plagioclase (py = pyroxene, phl = phlogopite, hb = hornblende, plag = plagioclase).

consists of euhedral, long, twinned prisms with faint optical zoning and is replaced by secondary hornblende and phlogopite. Other than primary magmatic hornblende, uralite replacing clinopyroxene as well as actinolitic hornblende developing from clinopyroxene and secondary hornblende are also present.

The primary phlogopitic mica is the essential mineral of the phlogopite gabbro, although phlogopite, replacing hornblende, is present in variable amounts and grain sizes in other gabbro types. Relict hornblende occurs locally within phlogopite crystals (Fig. 3B). The phlogopitic mica is strongly pleochroic and forms large flakes (Figs. 3A and 3B), and shows bright interference colors of the second and third orders, with a low 2V of 2–8°. As a result of weathering, phlogopite is transformed to vermiculite at rims and along cleavage planes (Toksoy and Öner, 1997; Toksoy, 1998). Because of oxidation during vermiculitization, the primary micas have high relief and include numerous tiny iron oxide grains along fracture and cleavage planes. Vermiculite replacing phlogopite plates shows optical continuity with the parent mineral. It is colorless to pale yellow with very weak interference colors.

Plagioclase is present in almost all gabbro types, but is limited in the phlogopite gabbro and pyroxene-phlogopite gabbro with a mode of up to 10%. However, plagioclase accounts for 90% of the modal mineralogy in plagioclase-rich, leucocratic parts of the plagioclase-hornblende gabbro and/or hornblende-plagioclase gabbro. The composition of plagioclase ranges from labradorite to bytownite (An_{50-70}). Plagioclase has euhedral to anhedral forms, and is in subophitic relation to pyroxene and hornblende. As a result of alteration, secondary plagioclase development—with higher albite content at the rims—and sericite also are present in and around plagioclase crystals. Neither olivine nor orthopyroxene (or related pseudomorphs) is present in the Kurancali metagabbro.

Petrology

Analytical techniques

Twelve representative gabbro samples were ground and concentrated by handpicking. Since this method did not yield pure mineral samples, separated samples were wet ground, and fully dispersed in distilled water by shaking and ultrasonic treatment. Dried samples were sieved to the range of 90–150 μm for subsequent mineral separation in a Frantz isodynamic magnetic separator. As a result of this separation process, almost pure mica samples from 8 hand specimens were obtained. Moreover, the purity of two clinopyroxene samples and two amphibole samples was estimated to be more than 95%.

Chemical analyses of seven mineral separates from the vermiculite-bearing phlogopite gabbro, pyroxene gabbro, and hornblende gabbro were performed using the standard inductively coupled plasma spectrometry (ICP) method in an automated PERKIN ELMER Optima 2000 instrument at Toprak Seniteri ve Izolator Sanayii A.S. Eskisehir Karo Fabrikasi, Eskisehir, Turkey (Table 1). Since the total iron is reported as Fe_2O_3 by ICP, the same samples were decomposed in an orthophenanthroline complex to allocate ICP total-iron values to Fe^{2+} and Fe^{3+}. Fe^{2+} was measured colorimetrically in the prepared complex using the Unicam SP 600 Series 2 spectrophotometer at the Department of Geological Engineering, Middle East Technical University. Purified mica samples were examined using a Rigaku Geiferflex X-ray diffractometry (XRD) unit, with Ni-filtered CuKα radiation at a voltage of 40 kV and current of 20 mV, at the General Directorate of Mineral Research and Exploration (MTA).

Chemical analyses of the constituent mineral separates (pyroxene, amphibole, and dark mica) were utilized in resolving the mineral nomenclature (Table 1). The unit-cell contents of the minerals were calculated using the method described by Deer et al. (1980), in which anhydrous forms of the amphiboles and micas have been assumed.

For whole-rock analysis, 15 gabbroic samples were collected. Eight were analyzed for major and selected trace elements (Table 2). All samples were analyzed on an ARL 8420 X-ray fluorescence spectrometer (Department of Earth Sciences, University of Keele, UK), calibrated against both international and internal Keele standards of appropriate composition. Details of methods, accuracy, and precision were given by Floyd and Castillo (1992).

Mineral chemistry

The obtained unit-cell contents of individual pyroxene analyses were plotted on the Wo-En-Fs diagram prepared by Morimoto et al. (1988) (Fig. 4A). According to these plots, the analyzed pyroxenes were defined as diopsidic ($En_{32}Fs_{19}Wo_{49}$–$En_{35}Fs_{18}Wo_{48}$). The pyroxenes of the Kurancali metagabbro are rich in CaO (>20 wt%), and poor in Na_2O (<0.5 wt%) and TiO_2 (<1 wt%).

The amphibole samples were interpreted and named using the classification and nomenclature of Leake (1978). The calculations were made on the basis of Leake's standard formula definition $[A_{0-1}B_2C^{vi}{}_5T^{iv}{}_8O_{22}(OH,F,Cl)_2]$. The values obtained fit well with the calcic amphibole group having $(Ca+Na)_B \geq 1.34$ and $Na_B < 0.67$. The studied samples plot in the tschermakitic hornblende area of the calcic amphiboles (Fig. 4B). The amphiboles of the hornblende gabbro have high TiO_2 (> 1.85 wt%) and Al_2O_3 (> 12 wt%).

Reddish brown to purplish greenish mica is classified as Mg-biotite (phlogopitic) by plotting the analytical data given in Table 1 on the Mg-$Fe^{2+}(Mn^{2+})$ – $R^{3+}(Al,Fe^{3+},Ti)$ diagram, described for trioctahedral micas by Foster (1960) (Fig. 4C). For nomenclature, the data were also plotted on the phlogopite-annite-siderophyllite-eastonite rectangular diagram of Deer et al. (1980). According to these plots, one of the dark micas has an Mg-rich biotite composition (close to the phlogopite area), whereas two of them plot in the phlogopite area, within the range of $phlogopite_{(57-70)}$–$annite_{(30-43)}$ (Fig. 4D). These data are in good accordance with the results of petrographic and X-ray diffractometric (XRD) analyses. XRD patterns of mica samples display strong reflections of a $2M_1$ polytype with some weak vermiculite and interstratified phlogopite/vermiculite reflections (Fig. 5).

Whole-rock chemistry

In addition to the mineral chemistry, whole-rock geochemical data from X-ray fluorescence (XRF) analyses are also presented for eight samples from the Kurancali metagabbro. Although the analyses of the Kurancali metagabbro are limited to eight samples (Table 2), it is possible to divide them into two chemical groups according to their Nb/Y ratios (Fig. 6A). The first group has the low Nb/Y ratio of subalkalic basalts, whereas the second group emerges as transitional to alkalic. Nb/Y ratios tend to change little with fractionation in the basalt composition

TABLE 1. ICP Analyses of Pyroxenes, Amphiboles, and Dark Micas within the Kurancali Metagabbro

	Pyroxenes		Amphiboles		Dark micas		
Sample no.	FT-26	FT-111	FT-66	FT-410	FT-32	FT-43	FT-59/B
SiO_2	48.65	47.90	44.27	44.08	41.11	39.10	38.35
Al_2O_3	7.73	8.16	12.97	12.01	13.89	15.89	15.86
TiO_2	0.9	0.99	1.87	1.89	2.81	2.63	2.86
FeO	10.1	9.8	9.86	11.63	11.23	13.67	10.62
Fe_2O_3	1.2	0.7	6.0	6.14	5.9	6.02	5.92
MgO	9.89	10.42	9.21	8.84	12.50	10.34	13.82
CaO	20.91	20.57	11.32	11.93	0.23	0.44	0.20
Na_2O	0.52	0.40	1.45	1.22	0.25	0.22	0.27
K_2O	0.09	0.11	1.64	1.21	8.91	8.39	8.77
LOI	0.23	0.15	0.78	0.27	2.65	2.67	2.80
Total	100.22	99.2	99.37	99.22	99.48	99.37	99.47
Si	1.832	1.811	6.453	6.465	5.955	5.826	5.693
Al^{iv}	–	–	1.547	1.535	2.045	2.174	2.307
Al^{vi}	0.330[2]	0.363[2]	0.682	0.541	0.327	0.206	0.433
Ti	0.026	0.028	0.205	0.209	0.306	0.506	0.315
Fe^{2+}	0.318	0.310	1.202	1.427	0.644	0.653	0.653
Fe^{3+}	0.034	0.020	0.675	0.679	1.361	1.662	1.302
Mg	0.555	0.587	2.000	1.932	2.698	2.239	3.019
Ca	0.844	0.833	1.769	1.874	0.036	0.069	0.032
Na	0.038	0.030	0.410	0.347	0.070	0.063	0.078
K	0.005	0.006	0.305	0.227	1.647	1.556	1.640
En	32.33	33.93	–	–	–	–	–
Fs	18.53	17.91	–	–	–	–	–
Wo	49.14	48.16	–	–	0.3352	0.4260	0.3013
$Fe^{2+}/(Fe^{2+}+Mg)$	0.3643	0.3456	–	–	–	–	–
$(Ca+Na)_B$	–	–	2	2	–	–	–
Na_B	–	–	0.2314	0.1256	–	–	–
$(Na+K)_A$	–	–	0.4834	0.449	–	–	–
Mg/(Mg + FeZ)	–	–	0.62	0.58	–	–	–

[1]En = 100 × Mg/(Mg + Fe^{2+} + Ca); Fs = 100 x Fe^{2+}/(Mg + Fe^{2+} + Ca); Wo = 100 x Mg/(Mg + Fe^{2+} + Ca); $(Ca + Na)_B$, Na_B, and $(Na + K)_A$ = numbers in the B and A sites of the standard formulae given by Leake (1978).
[2]$Al^{(t)}$, not Al^{vi}.

range, and hence it is concluded that these two groups record separate magmatic events.

The subalkalic metagabbros clearly plot in the island-arc tholeiite (IAT) field of various discrimination diagrams (Figs. 6A, 6C, and 6D). Multi-element spider diagrams normalized against mid-ocean ridge basalts (MORB) (Pearce, 1982) also show the characteristic pattern of island arcs, with significant enrichment of low-field-strength elements (LFSE) and depletion of high-field-strength elements (HFSE) (Fig. 6E). Although the enrichment of LFSE (apart from incompatible, immobile Th) may reflect alteration of the Kurancali metagabbros, notably the enhanced Th and reduced Nb, it still indicates that the first group of metagabbros are typical arc tholeiites.

The second group of metagabbros differs from the first group in having higher LFSE, Nb, Ce, Zr,

TABLE 2. Representative Analyses of the Metagabbro from the Kurancali Area

Samples:	KRC-1[1]	KRC-2[2]	KRC-3[1]	KRC-4[1]	KRC-5[1]	KRC-6[1]	KRC-7[2]	KRC-8[2]
SiO_2	41.2	47.51	40.71	42.27	42.57	43.75	45.97	44.14
TiO_2	1.46	0.75	1.74	1.45	1.3	1.04	1.16	1.11
Al_2O_3	17.27	6.14	14.08	16.48	12.13	12.81	15.17	15.37
Fe_2O_3t	15.66	13.95	13.80	13.39	9.92	10.35	11.93	14.07
MnO	0.24	0.23	0.17	0.2	0.21	0.2	0.3	0.23
MgO	5.5	9.75	10.93	8.65	9.98	10.91	5.49	6.30
CaO	14.42	18.65	12.65	14	15.17	17.12	11.63	11.07
Na_2O	1.57	0.88	1.56	1.52	1.12	1	2.15	2.54
K_2O	0.89	0.97	2.01	1.41	0.85	0.9	4.83	3.03
P_2O_5	0.31	0.15	0.04	0.02	0.04	0.05	0.25	0.08
LOI	0.64	1.23	1.45	0.66	1.67	1.79	0.47	1.79
Total	99.14	100.21	99.14	100.2	100.18	100.06	99.63	99.95
Ba	457	321	467	325	158	169	8927	1985
CeX[3]	31	20	21	27	11	10	208	68
Cl	90	3	329	106	–	71	217	385
Cr	129	283	47	71	55	448	24	44
Cu	115	60	44	69	17	19	34	24
Ga	19	12	15	19	18	13	20	21
LaX[3]	12	11	7	3	2	–	98	33
Nb	9	5	10	11	8	7	35	37
NdX[3]	21	21	21	–	–	–	–	28
Ni	19	79	24	23	56	22	31	23
Pb	9	16	14	17	13	13	20	15
Rb	17	41	39	19	18	13	157	71
S	107	103	217	836	–	–	141	168
Sr	547	200	321	475	453	368	1807	783
ThX[3]	2	10	4	5	4	1	16	16
V	525	379	635	560	523	368	270	406
Y	26	21	27	30	25	21	51	31
Zn	138	89	108	105	98	60	152	174
Zr	59	121	70	63	57	36	181	169

[1]Subalkalic.
[2]Alkalic.
[3]X = elements analyzed by X-ray fluorescence.

and Y contents but lower Ti contents. The second group clearly plots in the calc-alkaline basalt (CAB) field on the discrimination diagrams (Figs. 6B, 6C, and 6D). The relatively high Nb/Y concentrations of the samples suggest that a within-plate tectonic setting (oceanic-island basalt–OIB) is more likely than a CAB (Fig. 6A). N-MORB–normalized spider diagrams of the first and second groups of metagabbros are quite distinctive, the latter showing a greater degree of enrichment (Fig. 6E). The second-group metagabbro samples display three main features: (1) a greater degree of enrichment in LFSE (Sr, K, Rb, and especially Ba and Th) relative to HFSE; (2) reduced Nb relative to LFSE and Ti relative to the HFSE; and (3) Ce and P_2O_5 enrichment relative to Zr, TiO_2, and Y. Such variations in high LFSE/HFSE ratios and negative anomalies of Nb, Ta, and Ti are typical of all island-arc, calc-alkaline rocks (Pearce and Cann, 1973). The very distinctive Ba enrichment is a peculiar feature of the ultramafic xenoliths

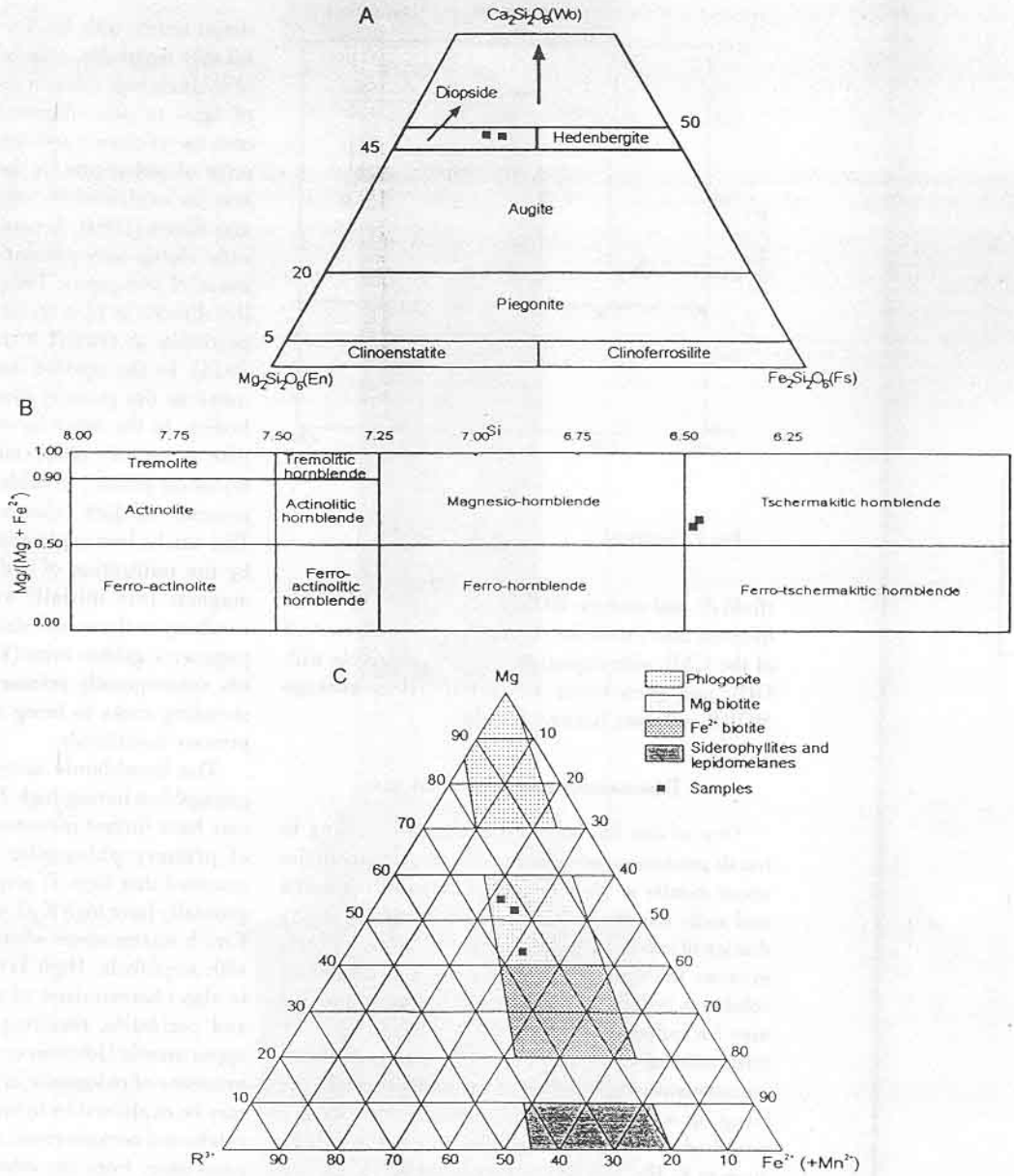

FIG. 4. Plots of (A) clinopyroxenes from the pyroxene-gabbro samples on the pyroxene quadrilateral diagram (after Morimoto et al., 1988); (B) amphibole samples on the Si and Mg/(Mg + Fe^{2+}) diagram for $(Ca + Na)_B > 1.34$, $Na_B < 0.67$ (Na + K)<0.50, and Ti<0.50 (after Leake, 1978); (C) dark mica samples on the triangular diagram showing relation between Mg, Fe^{2+} (Mn^{2+}), and R^{3+} (Al, Fe^{3+}, and Ti) in trioctahedral micas (after Foster, 1960); (D, on facing page) dark mica samples on the phlogopite-annite-eastonite-siderophyllite quadrilateral showing $Fe^{2+}/(Fe^{2+} + Mg)$ and Al^{IV} relation (after Deer et al., 1980).

from the Philippine arc system, which in extreme cases also contain cross-cutting veins with phlogopite (Maury et al., 1992). The chemical character of the CAB also is depicted in the comparative spider diagram of the second group, having higher Ba, Th, and Ce relative to the OIB (field c), backarc basalts

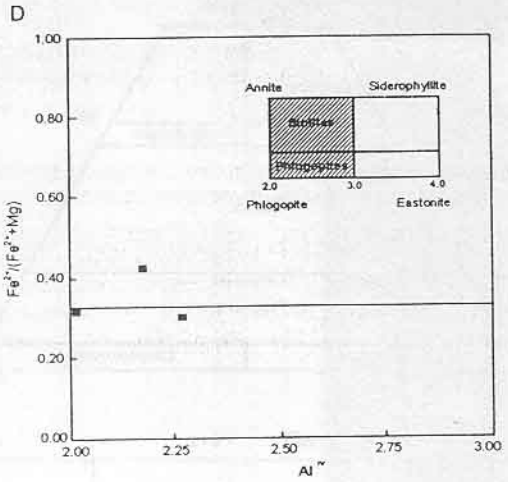

FIG. 4. Continued.

(field d), and average MORB (field e) (Fig. 6F). This diagram also shows the characteristic LFSE content of the CAB, with depletion values comparable with OIB, and even lower Ti contents than average MORB and some backarc basalts.

Discussion and Conclusions

One of the fundamental processes leading to basalt production and chemical heterogeneity in the upper mantle is the transport of volatile-rich fluids and melts into the overlying mantle wedge by dehydration of subducting slabs (Arculus, 1994, and references therein). By this process, the peridotite solidus is lowered and melting in the mantle wedge may be induced (Sekine and Wyllie, 1982). The infiltration of slab fluids and melts results in modal metasomatism by addition of hydrous phases in the hanging-wall mantle. The resulting rocks are enriched in large-ion lithophile elements (LILE) such as K, Rb, and Ba, and depleted in Nb, Ti, and Zr, typical of rocks associated with subduction-zone volcanism. The hydrous nature of the rocks, reflected in the abundance of phlogopite, further suggests an origin as part of a subduction-related plutonic complex.

The most characteristic feature of the Kurancali metagabbro is the presence of primary phlogopite. In terms of the phlogopite-annite series of biotite, phlogopites from the Kurancali metagabbro display a remarkably low $Fe^{2+}/(Fe^{2+} + Mg)$ ratio of 30–40. According to Rowins et al. (1991), biotite compositional trends with low $Fe^{2+}/(Fe^{2+} + Mg)$ are unmistakably magmatic, although the minor development of hydrous replacement indicates the limited extent of late- to post-magmatic fluid alteration. The absence of olivine and orthopyroxene, and the presence of phlogopite in the Kurancali metagabbro, may be explained by suggestions given by Hewitt and Wones (1984). According to them, siliceous liquids rising into peridotitic mantle precipitated zones of phlogopite. Phlogopite can either crystallize directly or by a reaction with olivine and orthopyroxene at crustal levels (Fyfe and McBirney, 1975). In the studied outcrops, phlogopite dominates as the primary phase in pegmatitic gabbro bodies. In the other layered gabbro types, phlogopite is mainly observed as a secondary phase replacing primary hornblende, as deduced from the presence of dark relict hornblende in phlogopite. This can be best explained by metasomatism caused by the infiltration of hydrous and LILE-enriched magmas into initially anhydrous gabbros, first resulting in the consolidation of phlogopite-bearing pegmatitic gabbro veins (Vidal et al., 1989). The fluids subsequently released diffused into the surrounding rocks to bring about the replacement of primary hornblende.

The hornblende samples from the Kurancali metagabbro having high Ti values (1.87–1.89 wt%) may have further importance for the documentation of primary phlogopite. Johnson et al. (1996) assumed that high-Ti amphiboles (0.82–3.66 wt%) generally have high K_2O, suggesting a transition to a K-rich environment where phlogopite might occur with amphibole. High Ti (>1.5 wt%) in amphiboles is also characteristic of the interaction of magma and peridotite, resulting in formation of hydrous upper mantle (Johnson et al., 1996). In this way, the existence of phlogopite in the Kurancali metagabbro may be explained by hybridization of magmas above subducted oceanic crust. All of these considerations point away from any other source or process (e.g., within-continental-plate alkaline magmatism, continental-rift-zone or continental basaltic magmatism) and toward a subduction-related setting for the Kurancali phlogopite gabbro. Nevertheless, phlogopite and high-K amphibole can be stabilized in the subduction environment at depths >110 km (Sudo and Tatsumi, 1990; Thompson, 1992; Davies, 1994). It has been shown through isotopic studies of Simcoe mantle xenoliths by Brandon et al. (1999) that the hybridized hanging-wall mantle may act for tens of millions of years as a reservoir for slab-

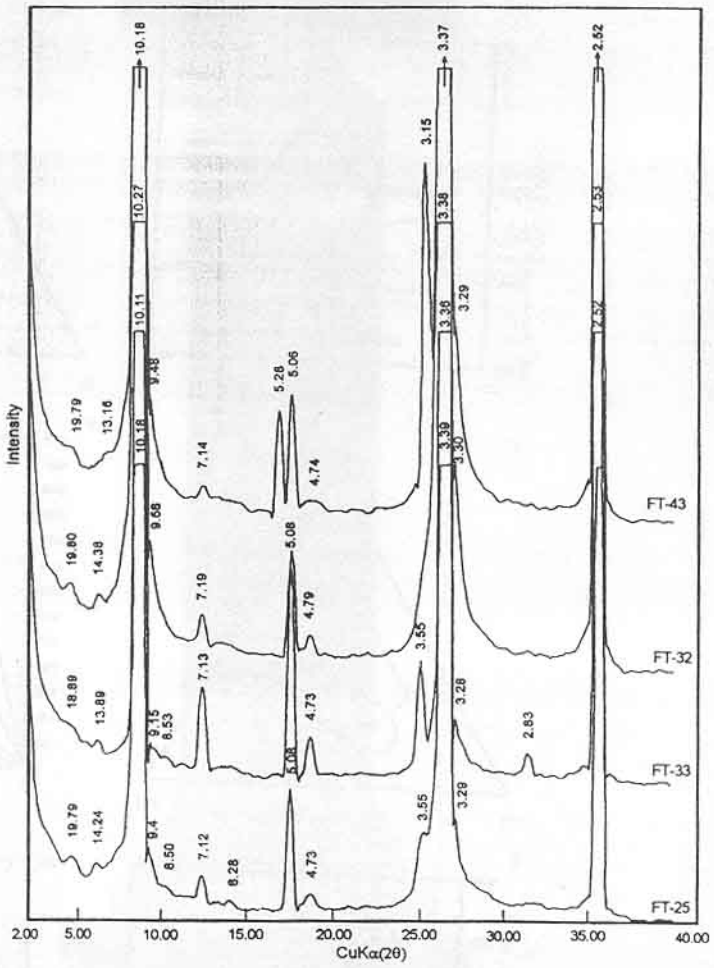

FIG. 5. X-ray diffractometry patterns of dark mica samples (air-dry patterns).

derived material. Therefore, in areas of regional convergence, a subduction-derived fluid component could be preserved and recycled by, for example, a later episode of magmatism related to rifting in backarcs, both in oceanic and continental crust. Thus, the presence of phlogopite alone is not a definitive indicator of the source area and the original tectonic setting of the Kurancali metagabbro.

Regional geological constraints, described in detail in Göncüoglu et al. (1992) and the overall geochemical features of the studied rocks argue against a continental-arc origin. However, these features alone are not sufficient for assigning them to one of the possible eruptive settings (either IAB-BAB or possibly OIB, taking into consideration the overall geochemical fingerprints but disregarding the presence of primary alkali-metasomatism). Therefore, we investigated the whole-rock geochemistry of the phlogopite-bearing rocks and compared them with better-studied mafic-ultramafic rocks in the CACC and elsewhere (e.g., OIB and MORB averages, mainly from Sun and McDonough, 1989; BABB [East Scotia Sea, Mariana Trough, Lau and North Fiji basins, Bransfield Strait], mainly from Saunders and Tarney, 1991), relative to their source compositions and derived melts (basalts).

The whole-rock geochemistry of the Kurancali metagabbro indicates the presence of two distinct groups. The first group has the characteristics of subalkalic basalts and is mainly represented by

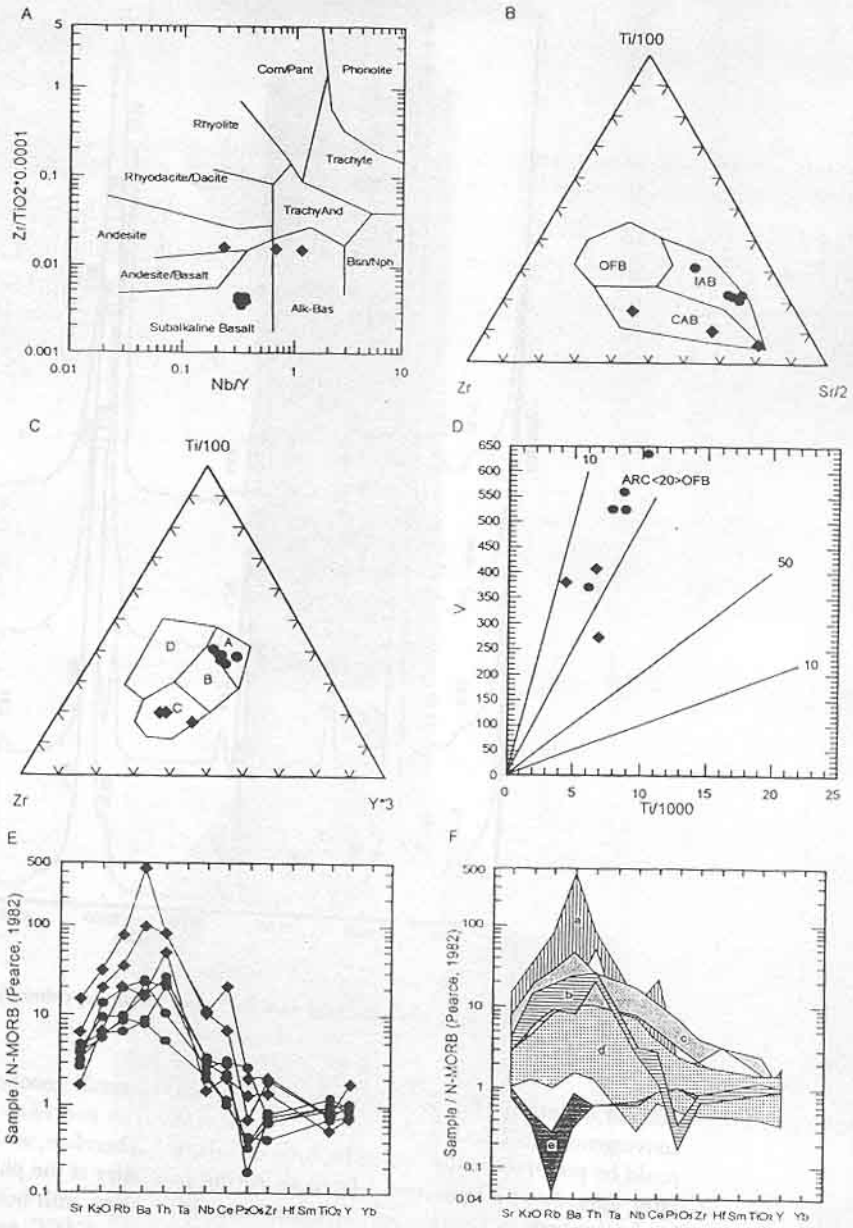

FIG. 6. Geochemical discrimination diagrams showing the distribution of the Kurancali metagabbro samples. Subalkalic and alkalic metagabbro groups are represented by darkened circles and diamonds, respectively. A. Nb/Y versus Zr/TiO_2 (after Winchester and Floyd, 1977). B. Ti-Zr-Sr (after Pearce and Cann, 1973): OFB = ocean-floor basalts (MORB); CAB = calc-alkaline basalts; IAB = island-arc tholeiites. C. Ti-Zr-Y (after Pearce and Cann, 1973): A = island-arc tholeiites; B = MORB, island-arc tholeiites, calc-alkali basalts; C = calc-alkali basalts; D = within-plate basalts. D. Ti versus V (after Shervais, 1982). E. MORB-normalized spider diagrams for different groups (normalization factors after Pearce, 1982). F. Comparative spider diagram of the groups (fields a and b) with well-known tectonic settings: Data taken from OIB (field c) and MORB (field e) averages mainly from Sun and McDonough (1989); backarc basin basalts (field d) (East Scotia Sea, Marianas Trough, Lau and North Fiji basins, Bransfield Strait) mainly from Saunders and Tarney (1991).

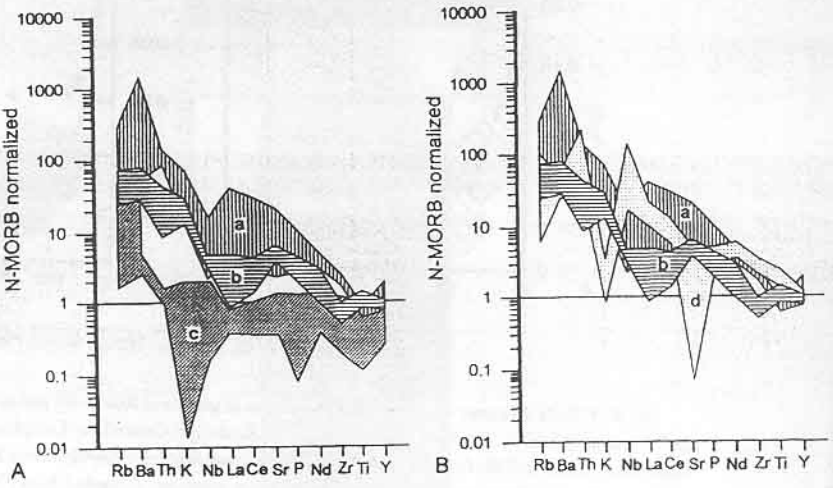

FIG. 7. Spider diagrams comparing the pegmatitic (field a) and the layered (field b) gabbro groups of Kurancali metagabbro with (A) stratiform and remnant ophiolitic fragments from the Central Anatolian Crystalline Complex in central Turkey (field c) (compiled from Floyd et al., 2000) and (B) Ankara Mélange metabasites (field d) (compiled from Floyd et al., 2000).

pyroxene and hornblende gabbros, whereas the second group, consisting mainly of pegmatitic phlogopite gabbros, emerges as transitional to alkalic. A distinct "subduction component" is manifested in both groups. The first group shows features characteristic of an island arc and plots in the IAT field of the discrimination diagrams (Figs. 6B–6E). The second group, with its greater degree of LFSE enrichment, has both OIB and CAB characteristics. However, as shown in Figure 6F, it has higher Ba, Th, and Ce and lower HFSE relative to OIB, a geochemical signature that is characteristic of island-arc calc-alkaline rocks (Pearce et al., 1994). The enrichment in LFSE and/or LILE is now widely attributed to metasomatism of a sub-arc magma source due to transfer of melt or fluid from the subducting oceanic crust, whereas the relative depletion of HFSE may be attributed either to their retention in refractory slab minerals or to their low solubility in the transporting fluids (e.g., Noll et al., 1996).

A geochemical comparison of the Kurancali metagabbro with other mafic-ultramafic bodies in central Anatolia is presented in Figures 7 and 8. The first group (Fig. 7A, field c) comprises samples from the gabbros, the dikes, and the volcanic section of the stratiform and remnant ophiolitic bodies of the CAO (e.g., Çiçekdag, Sarikaraman, and structurally isolated outcrops with suspected ophiolitic affinities; Yaliniz et al., 1996, 2000; Floyd et al., 2000). They exhibit features typical of supra-subduction-zone (SSZ) ophiolites and can be directly compared with other SSZ-type ophiolites from the Neotethyan zone (e.g. Pindos, Troodos, Oman; Yaliniz et al., 1996). The second group (Fig. 7B, field d) on the comparative diagram comprises alkalic basalts of OIB character in the Ankara Mélange that are comparable to the OIB of St. Helena (Floyd, 1993; Floyd et al., 2000).

From the comparative spider diagrams (Fig. 7), it is obvious that Kurancali metagabbro rocks are quite different than the better-studied rock groups of the CAO and the Ankara Mélange. They differ from the bulk of the stratiform and remnant ophiolitic bodies (Çiçekdag, Sarikaraman, etc.) in their relative enrichment in LILE, incompatible LFSE, and especially in HFSE. The studied rocks differ from the OIB-type rocks of the Ankara Mélange not only in their relative enrichment in LILE (mainly Ba and K) and depletion in Nb, but also in relative depletion in some HFSE (e.g., Nd, Zr and Ti).

The difference between the main groups of mafic/ultramafic rocks in central Anatolia and the studied rocks is also clearly demonstrated on the V/Ti-Zr diagram (Fig. 8A). In this diagram, the layered (host) gabbro samples from the Kuruncali area plot in the transition zone between BABB and IAB, whereas the phlogopite-rich pegmatitic gabbro samples plot in the IAB field. Both Kurancali groups are

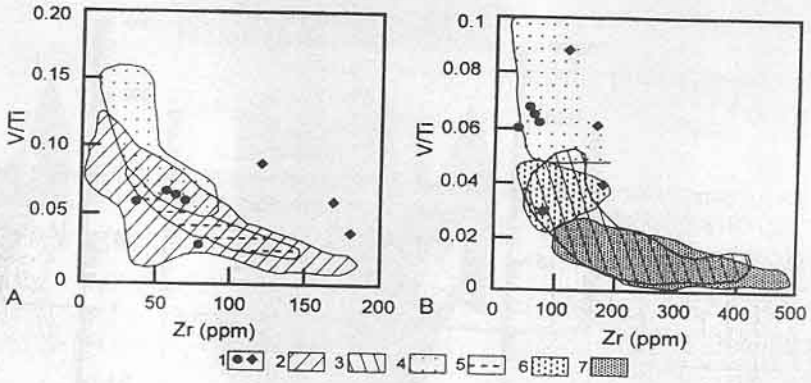

FIG. 8. V/Ti-Zr diagrams comparing data for different groups of Kurancali metagabbro with (A) the field of stratiform and remnant ophiolitic fragments from the Central Anatolian Crystalline Complex in Central Turkey (compiled from Floyd et al., 2000) and (B) field of the Ankara Mélange metabasites (compiled from Floyd et al., 2000). Legend: 1 = plots of Kurancali metagabbro samples; 2 = field of ophiolite remnants compiled from Floyd et al. (2000); 3 = field of pillow lavas within Ankara mélange and metabasites Central Anatolian Crystalline Complex compiled from Floyd et al. (2000); 4 = field of island-arc basalts (IAB) from Woodhead et al. (1993); 5 = backarc basin basalt (BABB) fields from Woodhead et al. (1993); 6 = mid-ocean ridge basalts (N-MORB) from Floyd and Castillo (1992); 7 = representative oceanic-island basalts (OIB) are alkali basalts (AB) of St. Helena from Chaffrey et al. (1989). Symbols are the same as those in Figure 6.

far removed from the OIB-type basalts of the Ankara Mélange that have low V/Ti and high Zr contents (Fig. 8B).

In conclusion, based upon the presented whole-rock geochemical data, together with the mineralogical composition of the Kurancali metagabbros, we suggest that these rocks were generated in a supra-subduction zone environment. They display geochemical features of transitional BABB/IAB- and IAB-type oceanic crust. A comparison with other ophiolitic successions in central Anatolia and elsewhere revealed that they are extremely enriched in LIL elements, indicative of alkaline metasomatism in the source region. Rocks with similar features are described from modern island-arc basements (e.g., Hamilton, 1994; Pearce et al., 1994). Hence, we suggest that the Kurancali metagabbro may represent the basement of an initial island arc, generated in a supra-subduction zone setting within the Izmir-Ankara branch of Neotethys. In previous studies (Göncüoglu and Türeli, 1993; Yaliniz et al., 1996, 2000; Floyd et al., 1998, 2000; Yaliniz and Göncüoglu, 1998), it was suggested that the allochthonous ophiolitic slivers represent uncoupled or different obducted slices of oceanic crust from a broad SSZ-type setting. If our preliminary suggestion is supported by detailed REE and isotope data, it is likely that slivers of an initial arc along with other (IAB and IAB/BABB) SSZ-type ophiolites were emplaced on the passive margin of the Tauride-Anatolide platform during the Late Cretaceous closure of the Izmir-Ankara branch of Neotethys.

Acknowledgments

The authors thank the BAYG and YDABCAG groups of the Scientific and Technical Research Council of Turkey (BAYG-TÜBITAK), for research support; and Miss Serap Içoz of the General Directorate of Mineral Research and Exploration, Mr. Celal Sahin of Toprak Seniteri ve Izolator Sanayi A.S. Eskisehir Karo Fabrikasi, and Prof. J.A. Winchester of the Department of Earth Sciences, University of Keele, UK for providing mineral, whole-rock, and trace-element analyses. Dr. R. Hébert and an anonymous reviewer are gratefully acknowledged for their expert comments that greatly improved an earlier version of this manuscript.

REFERENCES

Arculus, R. J., 1994, Aspects of magma genesis in arcs: Lithos, v. 33, p. 189–208.

Brandon, A. D., Becker, H., Carlson, R. W., and Steven, B. S., 1999, Isotopic constraints on time scales and mechanisms of slab material transport in the mantle wedge: Evidence from the Simcoe mantle xenoliths,

Washington, USA: Chemical Geology, v. 160, p. 387–407.

Chaffrey, D. J., Cliff, R. A., and Wilson, B. M., 1989, Characterisation of the St. Helena magma source, *in* Saunders, A. D., and Norry, M. J., eds., Magmatism in ocean basins: Geological Society of London, Special Publication, no. 42, p. 257–276.

Davies, J. H., 1994, Lateral water transport across a dynamic mantle wedge: A model for subduction zone magmatism, *in* Ryan, M. P., ed., Magmatic systems: New York, Academic Press, p. 197–221.

Deer, W. A., Howie, R. A., and Zussman, J., 1980, An introduction to rock forming minerals, 12th ed.: London, Longman, 528 p.

Floyd, P. A., 1993, Geochemical discrimination and petrogenesis of alkalic basalt sequences in part of the Ankara Mélange, central Turkey: Journal of the Geological Society of London, v. 150, p. 541–550.

Floyd, P. A., and Castillo, P. R., 1992, Geochemistry and petrogenesis of Jurassic ocean crust basalts, ODP Leg 129, Site 801, *in* Larson, R., Launcelot, Y. et al., eds., Scientific results: Proceedings of ODP, v. 129, p. 361–388.

Floyd, P. A., Göncüoglu, M. C., Winchester, J. A., and Yaliniz, M. K., 2000, Geochemical character and tectonic environment of Neotethyan ophiolitic fragments and metabasites in the Central Anatolian Crystalline Complex, Turkey, *in* Bozkurt, E., Winchester, J. A., and Piper, J. D. A., eds., Tectonics and magmatism in Turkey and the surrounding area: Geological Society of London, Special Publication, n. 173, p. 183–202.

Floyd, P. A., Yaliniz, M. K., and Göncüoglu, M. C., 1998, Geochemistry and petrogenesis of intrusive and extrusive ophiolitic plagiogranites, Central Anatolian Crystalline Complex, Turkey: Lithos, v. 42, p. 225–241.

Foster, M. D., 1960, Interpretation of the composition of trioctahedral micas: U.S. Geological Survey Professional Paper, v. 354-B, p. 11–49.

Fyfe, W., and McBirney, A. R., 1975, Subduction and the structure of andesite volcanic belts: American Journal of Science, v. 275A, p. 285–297.

Göncüoglu, M. C., Erler, A., Toprak, V., Olgun, E., Yaliniz, K., Kuşçu, I., Koksal, S., and Dirik, K., 1993, Geology of the central part of the Central Anatolian Massif: Part III, Geological evolution of the Tertiary basin of the Central Kizilirmak: Unpubl. Report No: 3313, Turkish Petroleum Coorporation (in Turkish).

Göncüoglu, M. C., Erler, A., Toprak, V., Yaliniz, K., Olgun, E., and Rojay, B., 1992, Geology of the western part of the Central Anatolian Massif: Part II, central part: Unpubl. Report No: 3155, Turkish Petroleum Corporation (in Turkish).

Göncüoglu, M. C., Toprak, G. M. V., Kuscu, I., Erler, A., Olgun, E., 1991, Geology of the western part of the Central Anatolian Massif: Part II, southern part: Unpubl. Report No: 2909, Turkish Petroleum Corporation (in Turkish).

Göncüoglu, M. C., and Türeli, K., 1993, Petrology and geodynamic interpretation of plagiogranites from Central Anatolian ophiolites (Aksaray-Türkiye): Turkish Journal of Earth Science, v. 2, p. 195–203.

Göncüoglu, M. C., Yaliniz, M. K., Özgül, L., and Toksoy, F., 1998, Petrogenesis of the Central Anatolian Ophiolites: An approach to the evolution of the Izmir-Ankara-Erzincan oceanic branch: Unpubl. report, TÜBITAK (in Turkish with English abstract).

Hamilton, W. B., 1994, Subduction systems and magmatism, *in* Smelle, J. L., ed., Volcanism associated with extension of consuming plate margins: Geological Society of London, Special Publication, no. 81, p. 3–28.

Hawkesworth, C. J., and Norry, M. J., 1983, Continental basalts and mantle xenoliths: Nantwich, UK, Shiva Publications, 378 p.

Hewitt, D. A., and Wones, D. R., 1984, Experimental phase relations of the micas, *in* Bailey, S. W., ed., Micas: Mineralogical Society of America, Reviews in Mineralogy, v. 13, p. 201–256.

Johnson, K. E., Davis, A. M., and Brynzia, L. T., 1996, Contrasting styles of hydrous metasomatism in the upper mantle: An ion microprobe investigation: Geochimica et Cosmochimica Acta, v. 60, p. 1367–1385.

Kadioglu, Y. K., Ates, A., and Güleç, N., 1998, Structural interpretation of gabbroic rocks in Agaçören Granitoid, central Turkey: Field observations and aeromagnetic data: Geological Magazine, v. 135, p. 245–254.

Leake, B. E., 1978, Nomenclature of amphiboles: American Mineralogist, v. 63, p. 1023–1052.

Maury, R. C., Defant, M. J., and Joron, J. L., 1992, Metasomatism of the subarc mantle inferred from trace elements in Philippine xenoliths: Nature, v. 360, p. 661–663.

Morimoto, N., Fabries, J., Ferguson, A. K., Ginzburg, I. V., Ross, M., Seifert, F. A., Zussman, J., Aoki, K., and Gottardi, G., 1988, Nomenclature of pyroxenes: American Mineralogist, v. 73, p. 1123–1133.

Noll, P. D., Newsom, H., Leeman, W. P., and Ryan, I. G., 1996, The role of hydrothermal fluids in the production of subduction zone magmas: Evidence from siderophile and chalcophile trace elements and boron: Geochimica et Cosmochimica Acta, v. 60, p. 587–611.

Pearce, J. A., 1982, Trace element characteristic lavas from destructive plate boundaries, *in* Thorpe, R. S., ed., Andesites: Orogenic andesites and related rocks: Chichester, UK, Wiley, p. 525–548.

Pearce, J. A., and Cann, J. R., 1973, Tectonic setting of basic volcanic rocks determined using trace element analysis: Earth and Planetary Sciences Letters, v. 19, p. 290–300.

Pearce, J. A., Ernewein, M., Bloomer, S. H., Parson, L. M., Murton, B. J., and Johnson, L. E., 1994, Geochemistry of Lau Basin volcanic rocks: Influence of ridge segmentation and arc proximity, *in* Smelle, J. L., ed., Vol-

canism associated with extension of consuming plate margins: Geological Society of London, Special Publication, no. 81, p. 53–75.

Rowins, S. M., Lalonde, A. E., and Cameron, E. M., 1991, Magmatic oxidation in the syenitic Murdock Creek intrusion, Kirkland Lake, Ontario: Evidence from the ferromagnesian silicates: Geological Journal, v. 99, p. 395–414.

Saunders, A. D., and Tarney, J., 1991, Back-arc basalts, *in* Floyd, P. A., ed., Oceanic basalts: Glasgow and New York, Blackie and Van Nostrand Reinhold, p. 219–264.

Sekine, T., and Wyllie, P. J., 1982, Phase relationships in the system $KAlSiO_4$–Mg_2SiO_4–SiO_2–H_2O as a model for hybridisation between hydrous siliceous melts and peridotite: Contributions to Mineralogy and Petrology, v. 79, p. 368–374.

Shervais, J. W., 1982, Ti-V plots and the petrogenesis of modern and ophiolitic lavas: Earth and Planetary Sciences Letters, v. 57, p. 101–118.

Sudo, A., and Tatsumi, Y., 1990, Phlogopite and K-amphibole in the upper mantle: Implication for magma genesis in subduction zones: Geophysical Research Letters, v. 17, p. 29–32.

Sun, S. S., and McDonough, W. F., 1989, Chemical and isotopic systematics of oceanic basalts: Implications for mantle composition and processes, *in* Saunders, A. D., and Norry, M. J., eds., Magmatism in ocean basins: Geological Society of London, Special Publication, no. 42, p. 313–345.

Thompson, A. B., 1992, Water in the Earth's upper mantle: Nature, v. 358, p. 295–302.

Toksoy, F., 1998, Petrography and mineralogy of the vermiculitized phlogopitic metagabbro from the Kurancali area (Kirsehir–Central Anatolia): Unpubl. M.Sc. thesis, Middle East Technical University, 175 p.

Toksoy, F., and Öner, A., 1997, Vermiculitization process, *in* Proceedings of 13th National Electron Microscopy Congress with International Participation, Ankara, Turkey, Sept. 1–4, 1997, p. 761–768.

Vidal, P., Dupuy, C., Maury, R., and Richard, M., 1989, Mantle metasomatism above subduction zones: Trace-element and radiogenic isotope characteristics of peridotite xenoliths from Batan Island (Philippines): Geology, v. 17, p. 1115–1118.

Winchester, J. A., and Floyd, P. A., 1977, Geochemical discrimination of different magma series and their differentiation products using immobile elements: Chemical Geology, v. 20, p. 325–343.

Woodhead, J., Eggins, S., and Gample, J., 1993, High field strength and transition element systematics in island arc and back-arc basin basalts: Evidence for multiphase melt extraction and a depleted mantle wedge: Earth and Planetary Science Letters, v. 114, p. 491–504.

Yaliniz, M. K., Floyd, P. A., and Göncüoglu, M. C., 1996, Supra-subduction zone ophiolites of Central Anatolia: Geochemical evidence from the Sarikaraman Ophiolite, Aksaray, Turkey: Mineralogical Magazine, v. 60, p. 697–710.

———, 2000, Geochemistry of volcanic rocks from the Cicekdag ophiolite, central Anatolia, Turkey, and their inferred tectonic setting within northern branch of the Neotethyan Ocean, *in* Bozkurt, E., Winchester, J. A., and Piper, J. D. A., eds., Tectonics and magmatism in Turkey and the surrounding area: Geological Society of London, Special Publication, no. 173, 203–218.

Yaliniz, M. K., and Göncüoglu, M. C., 1998, General geological characteristics and distribution of the Central Anatolian ophiolites: Hacettepe University Journal of Earth Science, v. 20, p. 19–30.

Yilmaz-Sahin, S., and Boztug, D., 1997, Petrography and whole-rock chemistry of the gabbroic, monzogranitic and syenitic rocks from the Çiçekdag region, N of Kirsehir, Central Anatolia, Turkey, *in* Boztug, D., Yilmaz-Sahin, S., Otlu, N., and Tatar, S., eds., Proceedings of the TÜBITAK-BAYG/NATO-D PROGRAM on Alkaline Magmatism (Theoretical Consideration and Field Excursion in Central Anatolia), 2–10 October, 1997, Department of Geology, Cumhuriyet University, Sivas-Turkey, p. 29–42.